

# Apolipoprotein E fragments present in Alzheimer's disease brains induce neurofibrillary tangle-like intracellular inclusions in neurons

Yadong Huang<sup>\*†‡§</sup>, Xiao Qin Liu<sup>†</sup>, Tony Wyss-Coray<sup>\*¶</sup>, Walter J. Brecht<sup>†</sup>, David A. Sanan<sup>†</sup>, and Robert W. Mahley<sup>\*†‡¶</sup>

<sup>\*</sup>Gladstone Institute of Neurological Disease and <sup>†</sup>Gladstone Institute of Cardiovascular Disease, P.O. Box 419100, San Francisco, CA 94141-9100; and Departments of <sup>‡</sup>Pathology, <sup>¶</sup>Neurology, and <sup>§</sup>Medicine, University of California, San Francisco, CA 94143

Contributed by Robert W. Mahley, May 22, 2001

**Human apolipoprotein (apo) E4, a major risk factor for Alzheimer's disease (AD), occurs in amyloid plaques and neurofibrillary tangles (NFTs) in AD brains; however, its role in the pathogenesis of these lesions is unclear. Here we demonstrate that carboxyl-terminal-truncated forms of apoE, which occur in AD brains and cultured neurons, induce intracellular NFT-like inclusions in neurons. These cytosolic inclusions were composed of phosphorylated tau, phosphorylated neurofilaments of high molecular weight, and truncated apoE. Truncated apoE4, especially apoE4( $\Delta$ 272–299), induced inclusions in up to 75% of transfected neuronal cells, but not in transfected nonneuronal cells. ApoE4 was more susceptible to truncation than apoE3 and resulted in much greater intracellular inclusion formation. These results suggest that apoE4 preferentially undergoes intracellular processing, creating a bioactive fragment that interacts with cytoskeletal components and induces NFT-like inclusions containing phosphorylated tau and phosphorylated neurofilaments of high molecular weight in neurons.**

**H**uman apolipoprotein (apo) E, a 34-kDa protein composed of 299 amino acids, occurs as three major isoforms, apoE2, apoE3, and apoE4 (1–3). ApoE4 has been linked to the pathogenesis of Alzheimer's disease (AD) (4–6). The apoE4 allele is a major risk factor or susceptibility gene associated with  $\approx$ 40–65% of cases of sporadic and familial AD, and it increases the occurrence and lowers the age of onset of the disease (7).

The neuropathological hallmarks of AD are the presence of extracellular amyloid plaques and intracellular neurofibrillary tangles (NFTs) in the brain (8–10). The plaques consist primarily of the amyloid  $\beta$  (A $\beta$ ) peptide (8–10), and the NFTs are composed largely of the highly phosphorylated microtubule-associated protein tau (p-tau) (9) and, to a lesser extent, phosphorylated neurofilaments of high molecular weight (p-NF-H) (11, 12). ApoE is a component of NFTs (4, 13, 14) and may be involved in the phosphorylation of tau (15), along with other components of the tangles, to form the cytosolic inclusions. Here we show that carboxyl-terminal-truncated fragments of apoE, especially apoE4( $\Delta$ 272–299), which is generated inside cultured neurons and in AD brains, interact with p-tau and p-NF-H and result in large, filamentous intracellular inclusions resembling NFTs in AD brains.

## Materials and Methods

**Antibodies.** Polyclonal goat anti-human apoE was from Calbiochem. Anti-carboxyl-terminal apoE (amino acids 272–299) was obtained by passing the polyclonal anti-apoE three times through a column that was prepared by binding a mixture of apoE3( $\Delta$ 272–299) and apoE4( $\Delta$ 272–299) to Sepharose CL-4B. The unbound fraction was used as anti-carboxyl-terminal apoE (amino acids 272–299). The bound fraction was used as anti-amino-terminal apoE (amino acids 1–271). Phosphorylation-dependent monoclonal tau antibodies, AT8 (p-Ser202), AT100 (p-Ser212 and p-Th214), AT180 (p-Th231), and AT270 (p-Th181), were from Endogen (Woburn, MA). Phosphorylation-dependent monoclonal NF-H antibodies, RT97 and SM-31, were

from Roche Molecular Biochemicals and Sternberger Monoclonals (Lutherville, MD), respectively.

**ApoE Expression Vectors.** PCR products encoding wild-type or modified forms of apoE3 or apoE4 were subcloned into a pFLAG-CMV-3 vector (Sigma) containing an amino-terminal FLAG fusion peptide and a preprotrypsin signal sequence or into a p-FLAG-CMV-4 vector (Sigma) containing an amino-terminal FLAG fusion peptide without a signal sequence. For some experiments, PCR products encoding wild-type or modified forms of apoE3 or apoE4 were subcloned into a pEGFP-C1 vector (CLONTECH) containing an amino-terminal green fluorescent protein (GFP) fusion without a signal sequence. In all cases, protein expression was driven with a human cytomegalovirus immediate-early promoter. All DNA constructs were confirmed by sequence analysis.

**Cell Cultures and Transfection.** Mouse neuroblastoma (Neuro-2a) cells (American Type Culture Collection) were maintained at 37°C in MEM containing 10% FBS. NT2 cells were kindly provided by S. Pleasure (University of California, San Francisco) and maintained in Opti-MEM-I (GIBCO) containing 5% FBS (16).

Primary cultures of cortical neurons were prepared from 17-day-old mouse embryos as described (17). Immunostaining of 6-day-old cortical cultures *in vitro* with cell-specific antibodies yields >90% neuron-specific enolase-immunoreactive cells (18).

Neuro-2a, NT2-N, or cultured mouse primary cortical neurons were transiently transfected with various apoE cDNA constructs by the Lipofectamine method. Transfected cells expressing similar levels of various forms of apoE3 or apoE4 (GFP-apoE3 or GFP-apoE4), as determined by anti-apoE immunofluorescent staining and/or flow cytometry, were used.

**Immunocytochemistry.** Neuro-2a cells were grown in two-well chamber slides for 24 h and transiently transfected with various apoE3 or apoE4 DNA constructs, as described above. After two washes in PBS, the transfected cells were fixed, permeabilized, and stained with different primary antibodies and FITC-, rodamine-, or Cy5-coupled secondary antibodies as described (19). The immunofluorescently labeled slides were mounted in VectaShield (Vector Laboratories) and viewed with an MRC-1024 laser scanning confocal system (Bio-Rad) mounted on an Optiphot-2 microscope (Nikon).

Abbreviations: apo, apolipoprotein; AD, Alzheimer's disease; NFT, neurofibrillary tangle; A $\beta$ , amyloid  $\beta$ ; p-tau, phosphorylated tau; p-NF-H, phosphorylated neurofilaments of high molecular weight; GFP, green fluorescent protein.

§To whom reprint requests should be addressed. E-mail: yhuang@gladstone.ucsf.edu.

The publication costs of this article were defrayed in part by page charge payment. This article must therefore be hereby marked "advertisement" in accordance with 18 U.S.C. §1734 solely to indicate this fact.

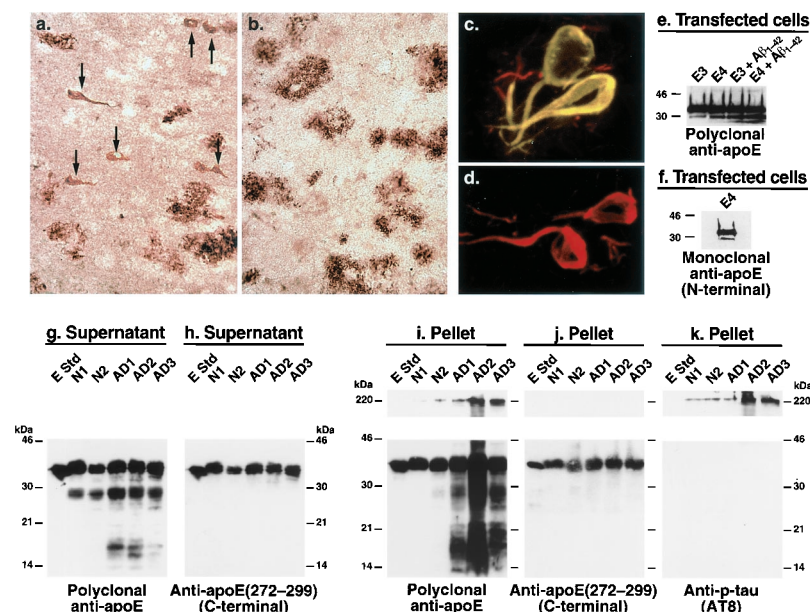


**Fig. 1.** Carboxyl-terminal-truncated forms of apoE accumulate in AD brains and NFTs. (*a* and *b*) Immunostaining of AD brain sections with anti-amino-terminal apoE (*a*) or anti-carboxyl-terminal apoE (*b*). (*c* and *d*) Double immunofluorescence staining of AD brain sections with anti-p-tau (red) and anti-amino-terminal apoE (green) (*c*) or anti-p-tau (red) and anti-carboxyl-terminal apoE (green) (*d*). (*e* and *f*) Neuro-2a cells expressing apoE3 or apoE4 were incubated with or without synthetic Aβ<sub>1-42</sub> (10 μM) for 24 h at 37°C. After incubation, cell lysates were immunoprecipitated with a monospecific polyclonal anti-apoE followed by Western blotting with polyclonal anti-apoE (*e*) or monoclonal anti-apoE (6C5) (*f*) that recognizes the first 15 amino acids of the amino terminus of apoE (45). (*g*–*k*) Brain tissues from two nondemented normal individuals (N1 and N2) and three AD patients (AD1, AD2, and AD3) were homogenized. Both the supernatants (*g* and *h*) and the solubilized pellets (*i*–*k*) were subjected to SDS/PAGE and analyzed by Western blotting with polyclonal antibodies against full-length apoE (*g* and *i*), the carboxyl terminus (amino acids 272–299) of apoE (*h* and *j*), or a mAb against p-tau (AT8) (*k*). E Std, apoE standard (200 ng protein). (Original magnifications: *a* and *b*, ×200; *c* and *d*, ×600.)

**Human Brain Tissues.** Brain tissues (cortex) from two normal subjects (N1, 97 years old, apoE3/3; N2, 69 years old, apoE3/3) without dementia, plaques, or NFTs in the brain and three AD patients (AD1, 77 years old, apoE4/2; AD2, 74 years old, apoE4/4; AD3, 76 years old, apoE4/3) with dementia, plaques, and NFTs in the brain were kindly provided by Eliezer Masliah (University of California at San Diego, La Jolla). Tissues were collected at 12, 9, 3, 10, and 5 h after death, respectively, frozen immediately on dry ice, and stored at –80°C until used.

Human cortical brain tissues (1–2 g) were homogenized with a Polytron homogenizer (75% power, 30 s × 4) in 1.5 ml of ice-cold lysis buffer I (50 mM Tris-HCl, pH 8.0/150 mM NaCl/0.1% SDS/0.5% Nonidet P-40/0.5% sodium deoxycholate and a mixture of protease inhibitors). After centrifugation at 25,000 *g* for 30 min at 4°C to obtain the solubilized proteins (supernatant), the pellet was further homogenized with a Polytron homogenizer (75% power, 30 s × 4) in 1.5 ml of ice-cold lysis buffer II (50 mM Tris-HCl, pH 8.0/150 mM NaCl/4% SDS/1% Nonidet P-40/1% sodium deoxycholate and a mixture of protease inhibitors). The supernatant and the solubilized pellet (200 μg total proteins) were subjected to SDS/PAGE and analyzed by Western blotting.

**Immunoprecipitation and Western Blotting.** Neuro-2a cells transiently transfected with apoE DNA constructs (24–48 h) were lysed in ice-cold lysis buffer III (50 mM Tris-HCl, pH 8.0/150 mM NaCl/0.1% SDS/1% Nonidet P-40/0.5% sodium deoxycholate and a mixture of protease inhibitors) for 30 min. After centrifugation in an Eppendorf centrifuge (13,000 rpm for 15 min), apoE in the supernatant was immunoprecipitated with monospecific goat anti-human apoE and protein-A agarose beads. The immunoprecipitates were then analyzed for apoE, p-tau, or p-NF-H by Western blotting with the corresponding antibodies. Alternatively, the supernatants of cell lysates were immunoprecipitated with monoclonal anti-p-tau or anti-p-NF-H and analyzed by Western blotting with anti-apoE.

**Electron Microscopy.** Neuro-2a cells transiently transfected with DNA constructs encoding GFP or GFP-apoE4(Δ272–299) were lifted from the plates with 0.05% trypsin and 0.05 mM EDTA. GFP-positive cells were sorted by a fluorescence-activated cell sorter and pelleted by centrifugation. The cells were fixed (2.5%

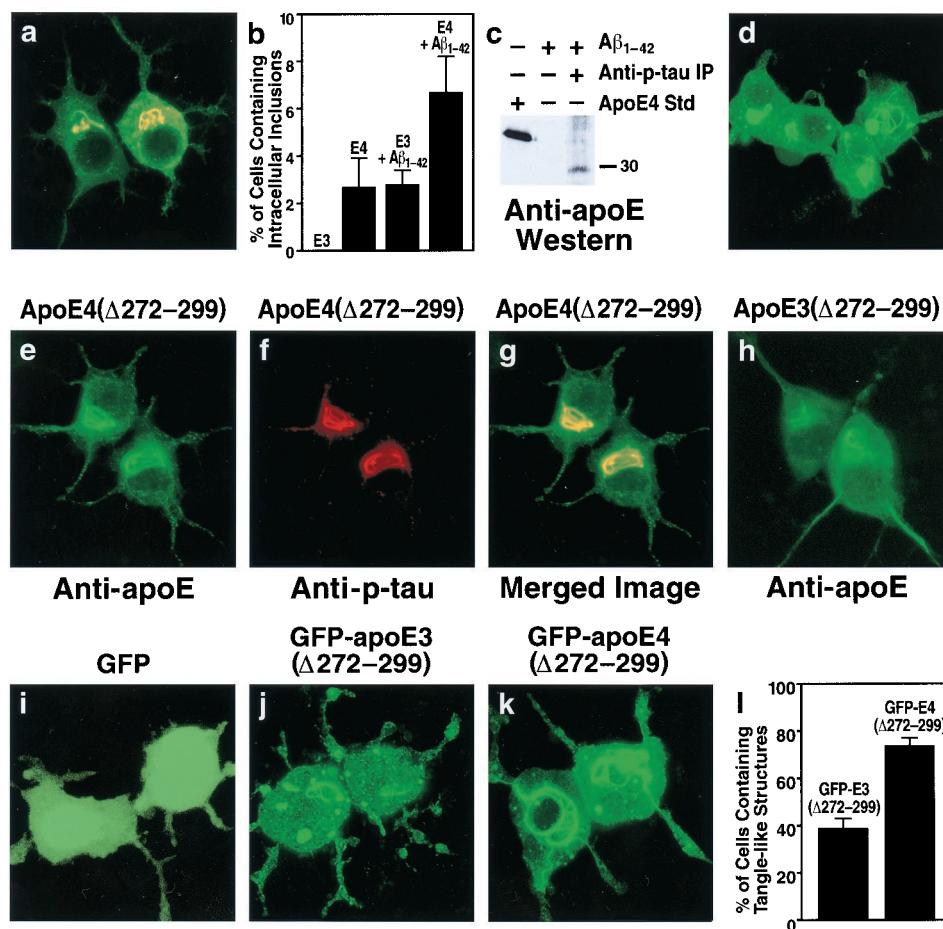
glutaraldehyde, 1 h; 2% OsO<sub>4</sub>, 1 h), dehydrated, embedded, sectioned, and stained with uranyl acetate and lead citrate. The cells then were photographed with a JEOL CCX-100II electron microscope.

## Results

**Carboxyl-Terminal-Truncated Forms of ApoE Accumulate in AD Brains and Are Associated with NFTs.** To characterize the apoE in AD plaques and NFTs, we immunostained AD brain sections with antibodies against various regions of apoE. Anti-amino-terminal apoE (amino acids 1–271) revealed both amyloid plaques and NFTs (Fig. 1*a*, arrows), whereas anti-carboxyl-terminal apoE (amino acids 272–299) revealed only amyloid plaques (Fig. 1*b*). The NFTs were double-immunolabeled with anti-p-tau and anti-amino-terminal apoE (Fig. 1*c*) but not with anti-carboxyl-terminal apoE (Fig. 1*d*). These results suggest that apoE exists in NFTs as a carboxyl-terminal-truncated form.

To confirm the presence of these forms of apoE in human brains, brain lysates from nondemented normal subjects and AD patients were analyzed by Western blotting. Anti-full-length apoE revealed not only full-length apoE but also a ≈29- to 30-kDa apoE fragment in the supernatant of brain lysates from both normal subjects and AD patients; however, the fragment occurred to a greater extent in AD brains (Fig. 1*g*). This fragment also was found in detergent-solubilized pellets from AD brains, which were enriched in plaques and NFTs, but not in the pellets from normal brains (Fig. 1*i*). Smaller apoE fragments (≈14–20 kDa) were found in both the supernatant and the solubilized pellet fractions of AD brains but not of nondemented normal brains (Fig. 1*g* and *i*). However, Western blotting with anti-carboxyl-terminal apoE revealed only full-length apoE in both the supernatant (Fig. 1*h*) and the solubilized pellet fractions (Fig. 1*j*), suggesting that the fragments are carboxyl-terminal-truncated forms of apoE. Large complexes (>220 kDa) were detected in the solubilized pellets of AD brains by anti-full-length apoE (Fig. 1*i*) and anti-p-tau (Fig. 1*k*) but not by anti-carboxyl-terminal apoE (Fig. 1*j*), suggesting that these large complexes contain carboxyl-terminal-truncated forms of apoE and p-tau. Thus, carboxyl-terminal-truncated forms of apoE accumulate in AD brains, form complexes with p-tau, and are associated with NFTs.

**Fig. 2.** Carboxyl-terminal-truncated apoE induces intracellular NFT-like inclusions in the cytosol of Neuro-2a cells. (a) Neuro-2a cells transiently transfected with apoE4 cDNA were double-immunostained with anti-apoE (green) and anti-p-tau (red) antibodies. This is representative of the cells containing apoE and p-tau immunoreactive intracellular inclusions (yellow) (more than 1,500 cells examined). (b) ApoE3- and apoE4-transfected Neuro-2a cells were incubated with or without 10  $\mu$ M synthetic A $\beta_{1-42}$  peptide at 37°C for 36 h. After incubation, the cells were double-immunostained with anti-apoE and anti-p-tau, and the percentage of transfected cells containing apoE and p-tau immunoreactive intracellular inclusions was calculated. Each column represents mean  $\pm$  SD of four experiments ( $P < 0.001$ , apoE4 versus apoE3 or apoE4 + A $\beta_{1-42}$  versus apoE3 + A $\beta_{1-42}$ ;  $>400$  transfected cells counted per experiment). (c) Cell lysates of apoE4-transfected Neuro-2a cells treated with A $\beta_{1-42}$  (10  $\mu$ M, 36 h) were immunoprecipitated with a monoclonal anti-p-tau (AT8 or AT270). Control lysates were not immunoprecipitated with anti-p-tau. Anti-apoE Western blotting revealed a band with a lower molecular mass than full-length apoE ( $\approx 29$ –30 kDa versus 34 kDa). (d) Neuro-2a cells were incubated for 30 h at 37°C with recombinant apoE4( $\Delta 272$ –299) (30  $\mu$ g/ml) complexed with rabbit  $\beta$ -very low density lipoproteins (20  $\mu$ g of protein/ml). After incubation, the cells were fixed and immunostained for apoE. (e–h) Neuro-2a cells transiently transfected with apoE4( $\Delta 272$ –299) (e–g) or apoE3( $\Delta 272$ –299) (h) cDNA were double-immunostained with anti-apoE (e) and anti-p-tau (f) antibodies or immunostained with anti-apoE alone (h). (g) Merged image of e and f. (i–k) Neuro-2a cells were transiently transfected with DNA constructs encoding GFP (i), GFP-apoE3( $\Delta 272$ –299) (j), or GFP-apoE4( $\Delta 272$ –299) (k). All three constructs lacked the sequence encoding the signal peptide, resulting in direct expression of GFP-apoE in the cytosol. After transfection, the percentage of transfected cells containing intracellular filamentous inclusions was calculated (l) (mean  $\pm$  SD of four experiments;  $>300$  transfected cells counted per experiment.  $P < 0.001$ , GFP-apoE4( $\Delta 272$ –299) versus GFP-apoE3( $\Delta 272$ –299). (Original magnification: a and d–k,  $\times 600$ ).



**Carboxyl-Terminal-Truncated ApoE Is Generated in Neuro-2a Cells.** The  $\approx 29$ - to 30-kDa band of apoE was also detectable in lysates of Neuro-2a cells expressing apoE3 or apoE4, with  $2.5 \pm 0.7$ -fold more being generated from apoE4 ( $P < 0.01$ ,  $n = 5$ ) than from apoE3 (Fig. 1e, left two lanes). Again, the  $\approx 29$ - to 30-kDa band represents a carboxyl-terminal-truncated form of apoE, as detected by a mAb, 6C5, that recognizes the first 15 amino-terminal amino acids of apoE (Fig. 1f). Furthermore, treatment of the transfected cells with the 42-aa form of A $\beta$  (A $\beta_{1-42}$ ) significantly increased the amounts of the carboxyl-terminal-truncated apoE3 and apoE4, with  $2.8 \pm 0.8$ -fold more being generated from apoE4 ( $P < 0.01$ ,  $n = 4$ ) (Fig. 1e, right two lanes). These results suggest that A $\beta_{1-42}$  activates an unknown proteolytic enzyme that cleaves apoE, especially apoE4, at its carboxyl terminus.

**ApoE4 Induces Intracellular Inclusions in Neuro-2a Cells.** In a subset ( $2.7 \pm 1.2\%$ ) of transfected cells expressing full-length apoE4 (Fig. 2b), apoE and p-tau immunoreactivity colocalized within intracellular inclusions (Fig. 2a). Immunostaining showed no intracellular inclusions in Neuro-2a cells expressing full-length apoE3 (Fig. 2b). However, treatment with A $\beta_{1-42}$  increased the number of apoE4-expressing cells containing apoE and p-tau immunoreactive intracellular inclusions ( $2.7 \pm 1.2\%$  to  $6.7 \pm 1.5\%$ ,  $P < 0.001$ ) and induced inclusions in a subset of apoE3-expressing cells (0 to  $2.8 \pm 0.6\%$ ,  $P < 0.001$ ) (Fig. 2b).

Importantly, anti-p-tau immunoprecipitation of cell lysates from A $\beta_{1-42}$ -treated cells expressing apoE4 and subsequent anti-apoE Western blotting revealed that the apoE4 in the complex was a truncated form with a molecular mass of  $\approx 29$ –30 kDa (Fig. 2c).

**Carboxyl-Terminal-Truncated ApoE Induces Intracellular NFT-Like Inclusions.** To determine whether carboxyl-terminal-truncated apoE induces intracellular NFT-like inclusions, we expressed apoE3 or apoE4 constructs possessing carboxyl-terminal truncations in Neuro-2a cells. Expression of apoE4 lacking the first 28 amino acids of the carboxyl terminus [apoE4( $\Delta 272$ –299)] resulted in intracellular NFT-like inclusions in  $78 \pm 8\%$  of transfected Neuro-2a cells (Fig. 2e). The inclusions were recognized by anti-p-tau (Fig. 2f), which colocalized with apoE (Fig. 2g), and anti-p-NF-H (data not shown). Expression of apoE3( $\Delta 272$ –299) also induced intracellular inclusions, but they were smaller (Fig. 2h) and occurred in significantly fewer cells ( $32 \pm 5\%$  versus  $78 \pm 8\%$ ,  $P < 0.001$ ). Importantly, exogenous apoE4( $\Delta 272$ –299), which had been complexed with  $\beta$ -very low density lipoproteins as a lipid transport vehicle and incubated with Neuro-2a cells, also induced intracellular NFT-like inclusions (Fig. 2d). Thus, both endogenously expressed and exogenously added apoE with the carboxyl-terminal truncation induced NFT-like inclusions in Neuro-2a cells. The truncated apoE probably escapes the secretory or the endosomal-lysosomal internalization pathway,

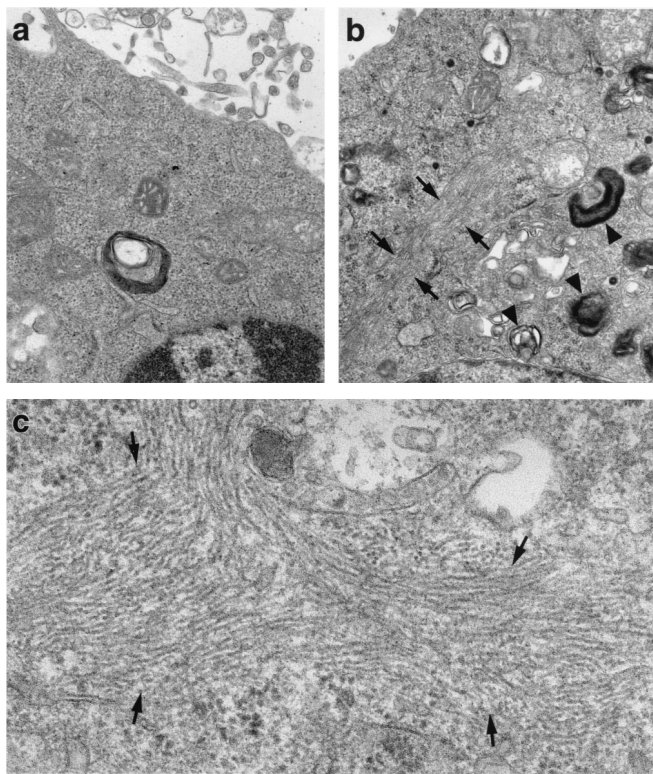


**Fig. 3.** Electron micrograph of the intracellular inclusions induced by GFP-apoE4( $\Delta 272-299$ ) in Neuro-2a cells. Neuro-2a cells were transiently transfected with GFP (a) or GFP-apoE4( $\Delta 272-299$ ) (b and c). GFP-positive cells were sorted with a fluorescence-activated cell sorter, pelleted by centrifugation, and examined with a JEOL CCX-100II electron microscope. (Original magnifications: a and b,  $\times 25,000$ ; c,  $\times 60,000$ .)

enters the cytosol, and interacts with p-tau and p-NF-H. There is evidence that apoE can appear in the cytosol of various cells (20–22), although another study failed to show this (23).

**Cytosolic ApoE( $\Delta 272-299$ ) Induces Intracellular NFT-Like Inclusions.** To interact with p-tau and p-NF-H, apoE must enter the cytosol. Therefore, we tested the hypothesis that cytosolic expression of apoE( $\Delta 272-299$ ) in Neuro-2a cells would enhance the formation of intracellular NFT-like inclusions. Indeed, expression of GFP-apoE4( $\Delta 272-299$ ) in the cytosol (construct lacked the sequence encoding the signal peptide) caused massive intracellular NFT-like inclusions in the cell bodies, occasionally extending into the neurites (Fig. 2 *k* and *l*), whereas GFP-apoE3( $\Delta 272-299$ ) expression resulted in many fewer intracellular inclusions (Fig. 2 *j* and *l*). GFP alone induced no inclusions (Fig. 2 *i*).

Expression of GFP-apoE4( $\Delta 272-299$ ) in the cytosol also induced intracellular NFT-like inclusions that were identified by double immunofluorescence staining with anti-apoE and anti-p-tau (AT8 or AT270) in primary cultured mouse cortical neurons and in human NT2 cells but not in nonneuronal cells (CHO, COS-7, C-6, HepG2, and McA-RH7777). Therefore, apoE4( $\Delta 272-299$ ) induces intracellular NFT-like inclusions only in neurons, consistent with the neuron-specific expression of tau and neurofilaments.

**Intracellular Inclusions in ApoE4( $\Delta 272-299$ )-Expressing Neuro-2a Cells Resemble NFTs in AD.** Ultrastructural analysis by electron microscopy showed large filamentous inclusions in Neuro-2a cells expressing cytosolic GFP-apoE4( $\Delta 272-299$ ) (Fig. 3*b*, arrows) but not in cells expressing GFP alone (Fig. 3*a*). The inclusions were composed of bundles of many straight filaments  $\approx 10-20$

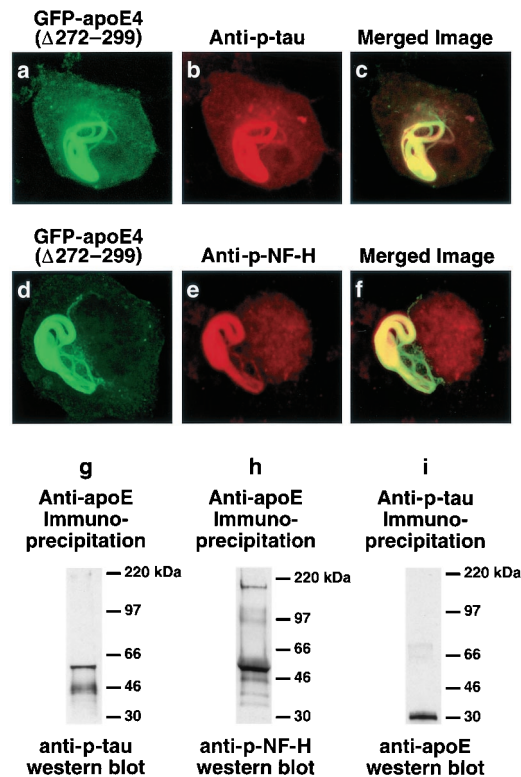


**Fig. 4.** Intracellular inclusions induced by GFP-apoE4( $\Delta 272-299$ ) in Neuro-2a cells contain p-tau and p-NF-H. (a–f) Neuro-2a cells transiently transfected with GFP-apoE4( $\Delta 272-299$ ) were immunostained for p-tau (AT270; similar results were obtained with AT8) or p-NF-H (e, SM31; similar results were obtained with RT97) and imaged by confocal microscopy. (c) Merged image of a and b. (f) Merged image of d and e. (g–i) Detection of a complex containing p-tau (g), p-NF-H (h), and truncated apoE (i) in Neuro-2a cells transiently transfected with apoE4( $\Delta 272-299$ ) after immunoprecipitation with anti-apoE (g and h) or anti-p-tau (AT8) (i) and Western blotting. (Original magnification: a–f,  $\times 600$ .)

nm in diameter (Fig. 3*c*, arrows), similar to the straight filaments in some NFTs in AD brains (24, 25). The filaments were randomly oriented and were not membrane-bound. Cells expressing GFP-apoE4( $\Delta 272-299$ ) also showed many electron-dense, membrane-bound organelles resembling autophagocytic vesicles containing damaged cell organelles (Fig. 3*b*, arrowheads).

Immunofluorescence staining of cells expressing cytosolic GFP-apoE4( $\Delta 272-299$ ) demonstrated that the inclusions contained p-tau, as detected by mAb AT8 (Fig. 4 *a–c*). However, the inclusions were variably positive for some (AT8+, AT100+, AT270+++), but not all (AT180–), of the mAbs that recognize p-tau in NFTs in AD brains, suggesting that some of the serines or threonines of tau were phosphorylated in the intracellular inclusions. The intracellular inclusion also contained p-NF-H as detected by mAb SM31 (Fig. 4 *d–f*) or RT97 (data not shown). The presence of both p-tau and p-NF-H in the intracellular inclusions was confirmed by immunoprecipitation studies and Western blotting with anti-p-tau, anti-p-NF-H, and anti-apoE (Fig. 4 *g–i*). These results suggest that apoE4( $\Delta 272-299$ )-induced intracellular filamentous inclusions have ultrastructural and biochemical characteristics resembling those of NFTs in AD brains.

**Amino Acids 245–260 of ApoE Interact with p-Tau and p-NF-H to Form Intracellular NFT-Like Inclusions.** To determine the region of apoE that mediated the interaction with p-tau and p-NF-H to form

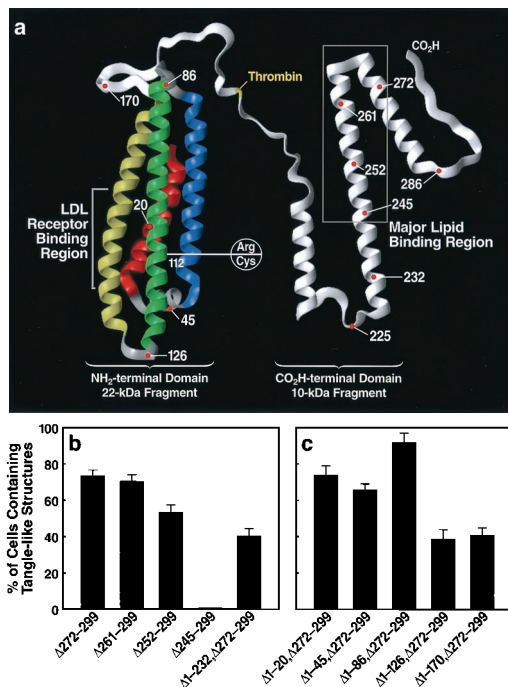


**Fig. 5.** The effects of deletions in the carboxyl- and amino-terminal domains of apoE on the formation of NFT-like structures in Neuro-2a cells. DNA constructs encoding fusion proteins of GFP and various carboxyl- or amino-terminal-truncated forms of apoE4 were prepared and transiently transfected into Neuro-2a cells. All constructs lacked the signal peptide sequence. (a) Model of apoE (modified from ref. 46) illustrating the structural regions where deletions were made and the polymorphic site (residue 112) that distinguishes apoE3 from apoE4. (b) Results defining amino acids 245–260 of apoE as critical for inclusion formation. (c) Deletion of helix 3 (amino acids 86–126) significantly reduced the ability of apoE4(Δ272–299) to form the intracellular inclusions ( $P < 0.001$ ). The percentages of cells containing NFT-like structures were determined (mean  $\pm$  SD of four experiments;  $>300$  transfected cells counted per experiment).

intracellular NFT-like inclusions, we transfected Neuro-2a cells with cDNA constructs encoding fusion proteins of GFP and apoE4 with carboxyl-terminal truncations of various lengths (lacking the signal sequence) (Fig. 5a). Expression of apoE4 with truncations to amino acid 261 [apoE4(Δ261–299)] or 252 [apoE4(Δ252–299)] did not affect the formation of intracellular NFT-like inclusions; however, truncation to amino acid 245 [apoE4(Δ245–299)] abolished formation of the NFT-like structures (Fig. 5b). These findings suggest that amino acids in the 245–260 region mediate the interaction with p-tau and p-NF-H to form the NFT-like inclusions in Neuro-2a cells. This conclusion was supported by the observation that the NFT-like inclusions also occurred in Neuro-2a cells transfected with a GFP-apoE cDNA construct encoding amino acids 233–271 of apoE [apoE(Δ1–232,Δ272–299)] (Fig. 5b).

**Amino-Terminal Domain Modifies the Ability of the Carboxyl-Terminal-Truncated ApoE4 to Form Intracellular NFT-Like Inclusions.** Because the sequence of amino acids 245–260 is identical in apoE3 and apoE4 (which differ only at residue 112) (Fig. 5a) and because apoE4(Δ272–299) has a greater ability to form the intracellular NFT-like inclusions than apoE3(Δ272–299) (Fig. 2l), the amino-terminal domain of apoE must modify the ability of apoE amino acids 245–260 to induce the inclusions. To test this hypothesis, we expressed GFP-tagged apoE4(Δ272–299) with a series of amino-terminal truncations in the cytosol of Neuro-2a cells and counted cells with intracellular inclusions. Removal of the first 20 amino acids

(Δ1–20,Δ272–299), the first  $\alpha$ -helix (Δ1–45,Δ272–299), or the first two  $\alpha$ -helices (Δ1–86,Δ272–299) did not alter the ability of GFP-apoE4(Δ272–299) to induce intracellular NFT-like inclusions (Fig. 5c). However, removal of the first three  $\alpha$ -helices (Δ1–126,Δ272–299) decreased GFP-apoE4(Δ272–299)-induced NFT-like inclusions by  $\approx 50\%$  (Fig. 5c). Removal of all four  $\alpha$ -helices (Δ1–170,Δ272–299) did not further decrease inclusion formation (Fig. 5c). These results suggest that the sequence in the third  $\alpha$ -helix (amino acids 86–126), which includes amino acid 112 (cysteine in apoE3 and arginine in apoE4) (Fig. 5a), modifies the ability of apoE4(Δ272–299) to induce intracellular NFT-like inclusions.

## Discussion

Several hypotheses have been advanced to explain the association of apoE with AD, including its role in altering  $A\beta$  deposition and clearance and plaque formation (26–30) and its effects on tau (31) and on the structure and function of the cytoskeleton (32–34). Our findings indicate that bioactive, carboxyl-terminal-truncated forms of apoE3 and apoE4 interact with cytosolic p-tau and p-NF-H to induce NFT-like inclusions in neuronal cells. Carboxyl-terminal-truncated apoE4 had a greater capacity to induce cytoskeletal alterations. NFTs composed of straight filaments are generated in neurons of transgenic mice expressing a mutant human tau (P301L) (35) but not in transgenic mice overexpressing wild-type human tau (36), suggesting that other factors, in addition to p-tau, are required to induce NFTs. Carboxyl-terminal-truncated apoE induced intracellular filamentous inclusions containing p-tau and p-NF-H even in the context of wild-type tau. Support for a role for apoE in NFT formation comes from pathological and epidemiological studies. ApoE is a component of NFTs (4, 13, 14), and most studies describe a gene dose-dependent effect of apoE4 on the number of NFTs in AD brains (37–40), although not all studies support this conclusion (41, 42).

Importantly, the carboxyl-terminal-truncated forms of apoE exist in NFTs and accumulate in the brains of AD patients. Detergent-solubilized pellet fractions from AD brain extracts were specifically enriched in apoE fragments, some of which were complexed with p-tau (Fig. 1i and k). Carboxyl-terminal-truncated apoE ( $\approx 29$ –30 kDa) also was found in neuronal cells incubated with exogenous apoE (data not shown) and in transfected neuronal cells that synthesized and secreted apoE (Fig. 1e and f). ApoE4 was much more susceptible to carboxyl-terminal truncation than apoE3, and  $A\beta_{1-42}$  treatment of the cells enhanced the generation of truncated apoE4 (Fig. 1e) and increased the number of cells with the intracellular NFT-like inclusions (compared with apoE3 plus  $A\beta_{1-42}$  treatment) (Fig. 2b). The identity of the putative protease that cleaves apoE at its carboxyl terminus is of great interest: it may serve as a therapeutic target for prevention and treatment of neurodegenerative diseases associated with apoE4.

The region of apoE responsible for its interaction with p-tau and p-NF-H to form the intracellular NFT-like inclusions includes amino acids  $\approx 245$ –260. This interaction occurred only when the apoE lacks the carboxyl-terminal  $\approx 30$  amino acids. Full-length apoE did not interact with p-tau and p-NF-H. However, any fragment of apoE possessing amino acids 245–260 but lacking the carboxyl-terminal amino acids also induced the NFT-like inclusions. Several carboxyl-terminal-truncated apoE fragments of different lengths were found in AD brains (Fig. 1g–j) and may be involved in the formation of NFTs.

Carboxyl-terminal-truncated apoE4 induced intracellular NFT-like inclusions containing p-tau and p-NF-H to a greater extent in neuronal cells than similarly truncated apoE3. However, both forms of apoE are identical with respect to amino acids 245–260; they differ only at residue 112. Therefore, the

amino-terminal domain of apoE appears to modulate the ability of the carboxyl-terminal-truncated fragments to induce intracellular NFT-like inclusions. Previously, the concept of domain interaction was proposed to explain alterations in the functional activity of apoE4 that distinguish it from apoE3 (43, 44). Domain interaction involving the amino terminus and carboxyl terminus of apoE4 is mediated by an ionic interaction between arginine-61 in the amino terminus (second  $\alpha$ -helix) and glutamic acid-255 in the carboxyl terminus (43, 44). However, deletion of the amino-terminal 86 amino acids, including arginine-61, from apoE4( $\Delta$ 272–299) did not affect its ability to form the intracellular NFT-like inclusions (Fig. 5c). On the other hand, deletion of the first three  $\alpha$ -helices ( $\Delta$ 1–126), including residue 112, which distinguishes apoE3 and apoE4, markedly reduced the ability of apoE4( $\Delta$ 272–299) to induce the intracellular inclusions. Thus, domain interaction

affecting this biologic activity appears to involve interactions other than arginine-61.

In conclusion, this study demonstrates that carboxyl-terminal-truncated fragments of apoE, which are generated in AD brains and cultured neurons, induce NFT-like inclusions in neuronal cells. Both quantitative and qualitative differences in the abilities of apoE4 and apoE3 to induce these inclusions could contribute to the increased susceptibility of human apoE4 carriers to AD and other types of central nervous system impairment.

We thank Dr. Karl Weisgraber for providing human apoE3 and apoE4 proteins and Dr. Zhong-Sheng Ji and Dennis Miranda for providing rabbit  $\beta$ -very low density lipoproteins. We also thank Sylvia Richmond and Karina Fantillo for manuscript preparation, Stephen Ordway and Gary Howard for editorial assistance, John C. W. Carroll and John Hull for graphics, and Stephen Gonzales and Chris Goodfellow for photography.

- Mahley, R. W. (1988) *Science* **240**, 622–630.
- Mahley, R. W. & Rall, S. C., Jr. (2001) in *The Metabolic and Molecular Bases of Inherited Disease*, eds. Scriver, C. R., Beaudet, A. L., Sly, W. S., Valle, D., Childs, B., Kinzler, K. W. & Vogelstein, B. (McGraw-Hill, New York), Vol. 2, pp. 2835–2862.
- Huang, Y. & Mahley, R. W. (1999) in *Plasma Lipids and Their Role in Disease*, eds. Barter, P. J. & Rye, K.-A. (Harwood, Amsterdam), pp. 257–284.
- Strittmatter, W. J., Saunders, A. M., Schmechel, D., Pericak-Vance, M., Enghild, J., Salvesen, G. S. & Roses, A. D. (1993) *Proc. Natl. Acad. Sci. USA* **90**, 1977–1981.
- Roses, A. D. (1994) *J. Neuropathol. Exp. Neurol.* **53**, 429–437.
- Mahley, R. W. & Rall, S. C., Jr. (2000) *Annu. Rev. Genomics Hum. Genet.* **1**, 507–537.
- Corder, E. H., Saunders, A. M., Strittmatter, W. J., Schmechel, D. E., Gaskell, P. C., Small, G. W., Roses, A. D., Haines, J. L. & Pericak-Vance, M. A. (1993) *Science* **261**, 921–923.
- Selkoe, D. J. (1991) *Neuron* **6**, 487–498.
- Crowther, R. A. (1993) *Curr. Opin. Struct. Biol.* **3**, 202–206.
- Roses, A. D. (1994) *Curr. Neurol.* **14**, 111–141.
- Smith, M. A., Rudnicka-Nawrot, M., Richey, P. L., Praprotnik, D., Mulvihill, P., Miller, C. A., Sayre, L. M. & Perry, G. (1995) *J. Neurochem.* **64**, 2660–2666.
- Vickers, J. C., Riederer, B. M., Marugg, R. A., Buée-Scherrer, V., Buée, L., Delacourte, A. & Morrison, J. H. (1994) *Neuroscience* **62**, 1–13.
- Namba, Y., Tomonaga, M., Kawasaki, H., Otomo, E. & Ikeda, K. (1991) *Brain Res.* **541**, 163–166.
- Wisniewski, T. & Frangione, B. (1992) *Neurosci. Lett.* **135**, 235–238.
- Tesseur, I., Van Dorpe, J., Spittaels, K., Van den Haute, C., Moechars, D. & Van Leuven, F. (2000) *Am. J. Pathol.* **156**, 951–964.
- Pleasure, S. J., Page, C. & Lee, V. M.-Y. (1992) *J. Neurosci.* **12**, 1802–1815.
- Fiumelli, H., Jabaudon, D., Magistretti, P. J. & Martin, J.-L. (1999) *Eur. J. Neurosci.* **11**, 1639–1646.
- Stella, N., Pellerin, L. & Magistretti, P. J. (1995) *J. Neurosci.* **15**, 3307–3317.
- Buttini, M., Orth, M., Bellosta, S., Akeefe, H., Pitas, R. E., Wyss-Coray, T., Mucke, L. & Mahley, R. W. (1999) *J. Neurosci.* **19**, 4867–4880.
- Hamilton, R. L., Wong, J. S., Guo, L. S. S., Krisans, S. & Havel, R. J. (1990) *J. Lipid Res.* **31**, 1589–1603.
- Han, S.-H., Einstein, G., Weisgraber, K. H., Strittmatter, W. J., Saunders, A. M., Pericak-Vance, M., Roses, A. D. & Schmechel, D. E. (1994) *J. Neuropathol. Exp. Neurol.* **53**, 535–544.
- Lovestone, S., Anderton, B. H., Hartley, K., Jensen, T. G. & Jorgensen, A. L. (1996) *NeuroReport* **7**, 1005–1008.
- DeMattos, R. B., Thorngate, F. E. & Williams, D. L. (1999) *J. Neurosci.* **19**, 2464–2473.
- Crowther, R. A. (1991) *Proc. Natl. Acad. Sci. USA* **88**, 2288–2292.
- Perry, G., Mulvihill, P., Manetto, V., Autilio-Gambetti, L. & Gambetti, P. (1987) *J. Neurosci.* **7**, 3736–3738.
- Strittmatter, W. J., Weisgraber, K. H., Huang, D. Y., Dong, L.-M., Salvesen, G. S., Pericak-Vance, M., Schmechel, D., Saunders, A. M., Goldgaber, D. & Roses, A. D. (1993) *Proc. Natl. Acad. Sci. USA* **90**, 8098–8102.
- Sanan, D. A., Weisgraber, K. H., Russell, S. J., Mahley, R. W., Huang, D., Saunders, A., Schmechel, D., Wisniewski, T., Frangione, B., Roses, A. D. & Strittmatter, W. J. (1994) *J. Clin. Invest.* **94**, 860–869.
- Ma, J., Yee, A., Brewer, H. B., Jr., Das, S. & Potter, H. (1994) *Nature (London)* **372**, 92–94.
- Wisniewski, T., Castaño, E. M., Golabek, A., Vogel, T. & Frangione, B. (1994) *Am. J. Pathol.* **145**, 1030–1035.
- LaDu, M. J., Falduto, M. T., Manelli, A. M., Reardon, C. A., Getz, G. S. & Frail, D. E. (1994) *J. Biol. Chem.* **269**, 23403–23406.
- Strittmatter, W. J., Saunders, A. M., Goedert, M., Weisgraber, K. H., Dong, L.-M., Jakes, R., Huang, D. Y., Pericak-Vance, M., Schmechel, D. & Roses, A. D. (1994) *Proc. Natl. Acad. Sci. USA* **91**, 11183–11186.
- Nathan, B. P., Bellosta, S., Sanan, D. A., Weisgraber, K. H., Mahley, R. W. & Pitas, R. E. (1994) *Science* **264**, 850–852.
- Nathan, B. P., Chang, K.-C., Bellosta, S., Brisch, E., Ge, N., Mahley, R. W. & Pitas, R. E. (1995) *J. Biol. Chem.* **270**, 19791–19799.
- Bellosta, S., Nathan, B. P., Orth, M., Dong, L.-M., Mahley, R. W. & Pitas, R. E. (1995) *J. Biol. Chem.* **270**, 27063–27071.
- Lewis, J., McGowan, E., Rockwood, J., Melrose, H., Nacharaju, P., Slegtenhorst, M. V., Gwinn-Hardy, K., Murphy, M. P., Baker, M., Yu, X., *et al.* (2000) *Nat. Genet.* **25**, 402–405.
- Ishihara, T., Hong, M., Zhang, B., Nakagawa, Y., Lee, M. K., Trojanowski, J. Q. & Lee, V. M.-Y. (1999) *Neuron* **24**, 751–762.
- März, W., Scharnagl, H., Kirça, M., Bohl, J., Groß, W. & Ohm, T. G. (1996) *Ann. N.Y. Acad. Sci.* **777**, 276–280.
- Morris, C. M., Benjamin, R., Leake, A., McArthur, F. K., Candy, J. M., Ince, P. G., Torvik, A., Bjertness, E. & Edwardson, J. A. (1995) *Neurosci. Lett.* **201**, 45–48.
- Nagy, Z., Esiri, M. M., Jobst, K. A., Johnston, C., Litchfield, S., Sim, E. & Smith, A. D. (1995) *Neuroscience* **69**, 757–761.
- Warzok, R. W., Kessler, C., Apel, G., Schwarz, A., Egensperger, R., Schreiber, D., Herbst, E. W., Wolf, E., Walther, R. & Walker, L. C. (1998) *Alzheimer Dis. Assoc. Disord.* **12**, 33–39.
- Heinonen, O., Lehtovirta, M., Soininen, H., Helisalmi, S., Mannermaa, A., Sorvari, H., Kosunen, O., Paljärvi, L., Ryyänen, M. & Riekinen, P. J., Sr. (1995) *Neurobiol. Aging* **16**, 505–513.
- Mukaetova-Ladinska, E. B., Harrington, C. R., Roth, M. & Wischik, C. M. (1997) *Dement. Geriatr. Cogn. Disord.* **8**, 288–295.
- Dong, L.-M. & Weisgraber, K. H. (1996) *J. Biol. Chem.* **271**, 19053–19057.
- Dong, L.-M., Wilson, C., Wardell, M. R., Simmons, T., Mahley, R. W., Weisgraber, K. H. & Agard, D. A. (1994) *J. Biol. Chem.* **269**, 22358–22365.
- Weisgraber, K. H., Rall, S. C., Jr., Mahley, R. W., Milne, R. W., Marcel, Y. L. & Sparrow, J. T. (1986) *J. Biol. Chem.* **261**, 2068–2076.
- Weisgraber, K. H. & Mahley, R. W. (1996) *FASEB J.* **10**, 1485–1494.